Acousto-optic couplings in a phoXonic crystal slab L_1 cavity

S Dupont[1,2,3], Q Rolland, J Gazalet[1,2,3], JC Kastelik[1,2,3]
[1]Univ Lille Nord de France, F-59000 Lille, France
[2]UVHC, IEMN-DOAE, F-59313 Valenciennes, France
[3]CNRS, UMR 8520, F-59650 Villeneuve d'Ascq, France

E-mail: samuel.dupont@univ-valenciennes.fr

Abstract. Acousto-optic coupling mechanisms within simultaneous photonic and phononic crystal cavities are theoretically studied. The structure considered is a silicon slab drilled periodically with air holes arranged on a square lattice; the cavity is obtained by removing one hole from the ideal crystal structure. Two acousto-optic coupling mechanisms are taken into account: the classical photo-elastic effect and the opto-mechanic effect which arises from the moving boundaries. The coupling mechanisms are computed according to the finite element method. The results reveal that the mechanisms can sustain each other or act with counteracted effects.

1. Introduction

Photonic and phononic crystals are artificial periodic structures that exhibit band gap phenomena for photons and phonons respectively [1, 2]. It is possible to design structures that enable the simultaneous confinement of both waves, the so-called phoxonic crystals. In these structures, due to the strong increase of energy localisation the acousto-optic coupling phenomenon are expected to be enhanced [3, 4]. A study of cavity mode coupling in two dimensions structures has evidenced an enhanced interaction with symmetric acoustic modes [6]. In this article, we study the modulation of optical cavity modes by acoustical cavity modes in a phoxonic crystal three dimensions structure: silicon slabs. Such a study is a step forward towards the understanding of technologically feasible structure behaviour. We investigate the dependence of the optical eigenmode frequency modulation on the spatial distribution and symmetry of the acoustic eigenmodes. The acousto-optic interaction strength is varying according to the couple of modes chosen. Two contributions are taken into account to compute the acousto-optic coupling: the classical photoelastic effect and the opto-mechanical effect; these two contributions act in different ways and their effects on the overall modulation can either sustain each other or in the contrary display counteracted effects. The computations are performed using the finite element method (FEM) for a 3D geometry consisting of a silicon slab drilled with periodic holes and surrounded by air. We first describe the phoxonic structure; we present the dispersion curves for the acoustic and optic waves and the acousto-optic coupling implementation. The most significant results are presented and discussed; we end up by some concluding remarks.

2. Model definition

2.1. Phoxonic bandgaps parameters

Content from this work may be used under the terms of the Creative Commons Attribution 3.0 licence. Any further distribution of this work must maintain attribution to the author(s) and the title of the work, journal citation and DOI.
Published under licence by IOP Publishing Ltd

The first step of the study consists in the determination of the dispersion curves for the photonic and phononic waves; such a study enables one to determine the occurrence of simultaneous photonic and phononic band gaps. Wide bandgaps are a prerequisite to promote the confinement of acoustic and optic waves. Recent investigations on silicon slabs have revealed that the couple of geometrical parameters of the reduced thickness (relative to the lattice parameter a) h / a = 0.6 and of the hole reduced radius r / a = 0.43, is a good candidate for the square lattice. It promotes the existence of quasi-TE, quasi-TM, shear and longitudinal vibrations [5].

2.2. Cavity acousto-optic coupling effects modeling

The cavity in such a structure consists in the absence of one hole (L_1 cavity): a point defect in the artificial crystal. Acoustical and optical modes are determined thanks to the supercell method: our calculations are based on a defect centred within a 9*9 supercell. The size of the supercell is slightly larger compared to our previous study considering 2D structures [6]; this ensures a good convergence of the computed modes. Due to geometrical considerations, the expected solutions are either symmetric or anti symmetric. This allows one to make use of a plane of appropriate symmetry midway between the two air/slab interfaces in order to reduce the computational power and memory requirements. So, the acoustical and optical modes are separated into symmetric and anti-symmetric ones, with respect to this horizontal symmetry plane. In what follows, we focus on the coupling between those modes due to the two contributing acousto-optic mechanisms.

We use the quasi-static approximation to compute the acousto-optic coupling effects owing to the several order of magnitude separating optical and acoustical angular frequencies. The acoustic cavity mode acts like a perturbation acting on the modulation of the optic cavity mode. That is, the optical mode is recalculated at different instants of an acoustical period. The two coexisting coupling mechanisms have different origins: the photo-elastic effect is due to the acoustic strain whereas the opto-mechanical effect is due to the geometrical deformations at the boundaries of the cavity. With the knowledge of acoustic cavity modes, one can determine the respective modulation resulting from both effects: the photo-elastic and the displacement of the hole air/silicon interfaces. The displacement field of the acoustic mode serves as input data to refine the boundaries of the optical cavity using the moving mesh method. The acoustic perturbation of the cavity is computed for sufficiently small time steps during one acoustic period. The strain field S_{kl} of the acoustic modes associated to the photo-elastic tensor ensures the computation of the photo-elastic effect to determine the refractive index spatial modulation according to:

$$\Delta\eta_{ij} = p_{ijkl} \cdot S_{kl} \tag{1}$$

with p_{ijkl} being the photoelastic constants of Silicon and η_{ij} the impermittivity tensor.

3. Results

We present the most significant results: dispersion curves of the slab, cavity modes and acousto-optic coupling in the cavity.

3.1. Band structure

Figure 1 displays the band structures along the Γ - X direction computed on the 9*9 supercell illustrated on the inset.

For clarity, black dotted lines are set at the bandgap edges of the corresponding perfect crystal (without the cavity). The band structure appears dense in the propagative region due to the band folding effect inherent to the supercell approach (in a 9*9 supercell, each dispersion curve folds 81 times). Moreover, the photonic band gap is filled with evanescent modes (from inside the light cone) that fold in the gap. We label the confined acoustic modes using capital letters and the optical cavity modes using Greek letters. Subscripts A and S stand for anti-symmetric and symmetric modes. Acoustic modes B_S, C_S and D_A, E_A are degenerated, as well as photonic modes γ_s, δ_s and β_a, γ_a. Compared to our previous 2D study [6], the acoustic eigenmodes exhibit a more complex

displacement spatial distribution; no breathing (fully symmetric) mode is found. We recall that the fully symmetric mode produces the highest coupling rates.

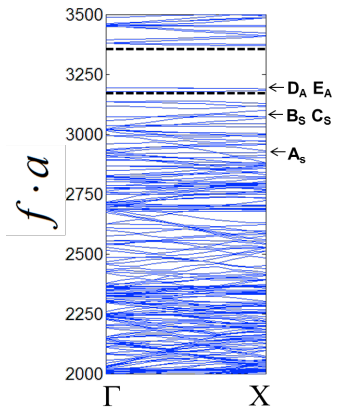

Figure 1.a Phononic band-structure of the supercell.

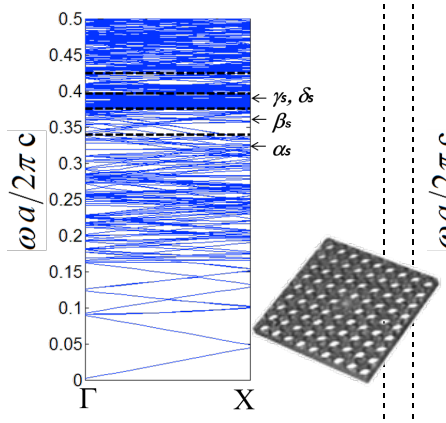

Figure 1.b Photonic band-structure of the supercell, symmetric modes.

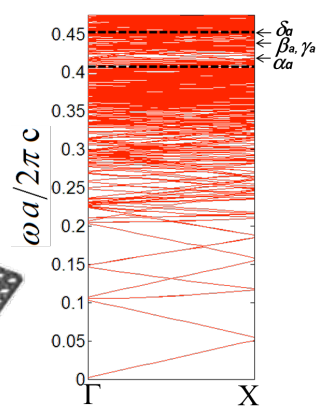

Figure 1.c Photonic band-structure of the supercell, anti-symmetric modes.

3.2. Cavity modes

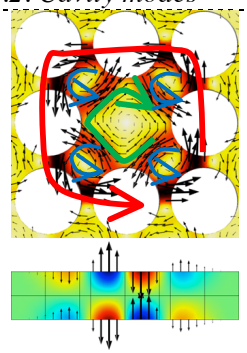

Figure 2.a Phononic A_S mode (top and side view).

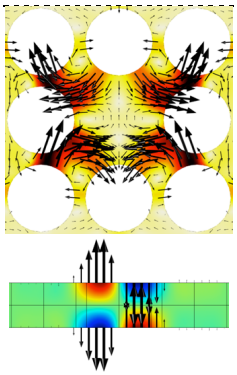

Figure 2.b Phononic B_S mode (top and side view).

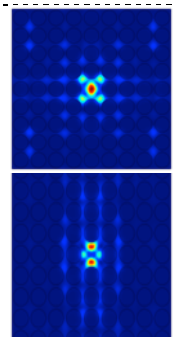

Figure 2.c Photonic modes α_a, β_a (top view).

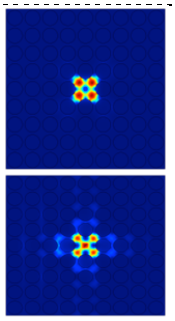

Figure 2.d Photonic modes α_s, β_s (top view).

The mode profiles are illustrated by figure 2 for the acoustic field (modes A_S and B_S, top figures are displayed in the (x, y) plane and bottom figures are displayed in the (y, z) plane) and for the electromagnetic energy (modes α_a, β_a and α_s, β_s). As highlighted by the added black arrows proportional to the displacement, the main displacements induced by the acoustic cavity modes are localized in and in the vicinity of the cavity: acoustic mode A_S corresponds to a rotation of the middle of the cavity associated with four local rotations of the corners of the cavity (green and blue bold arrows). During one half of the acoustic period, the rotation is clockwise and counter clockwise during the second half. With acoustic mode B_S the displacements are simpler to describe: both sides of the cavity are stretched and contracted one after the other, it results in an overall trapezoidal deformation of the cavity at $\Omega.t = \pi/2$ and $3.\pi/2$. Whereas, at $\Omega.t = 0$ and π the cavity is in its unperturbed shape.

3.3. Acousto-optic coupling

In figure 3, we plot the evolution of the optical mode eigenfrequencies as a function of an acoustic period. The green curves stand for the photo-elastic effect considered alone, the blue curves for the opto-mechanical effect alone and the red curves depict the evolution when both effects are taken into account simultaneously. We summarise the most significant trends observed in what follows:

- The two acousto-optic mechanism contributions can be in phase and sustain each other, or out of phase and act with counteracted effects. Consider for example the modulation of the optical mode β_A with the acoustic modes A_S and B_S: the photo-elastic contribution (green curve) is quite similar in both cases while the opto-mechanic contribution (blue curve) is in or out of phase, the global modulation (red curve) being respectively enhanced or reduced. Moreover, we note that the computation of both effects simultaneously results in an overall frequency modulation that is not equal to the algebraic sum of the modulations when the effects are computed separately.
- The frequency modulation of optical modes evolves at twice the acoustic frequency, this is compatible with an interpretation based on the perturbation theory: none of the acoustic modes is found to be even as regards all symmetry elements of the cavity, first order corrections vanish [7, 8].
- Higher values of frequency modulation due to photo-elastic effect and opto-mechanic effect are found when the overlap of the optical field with respectively the strain distribution and the cavity boundaries is maximised.

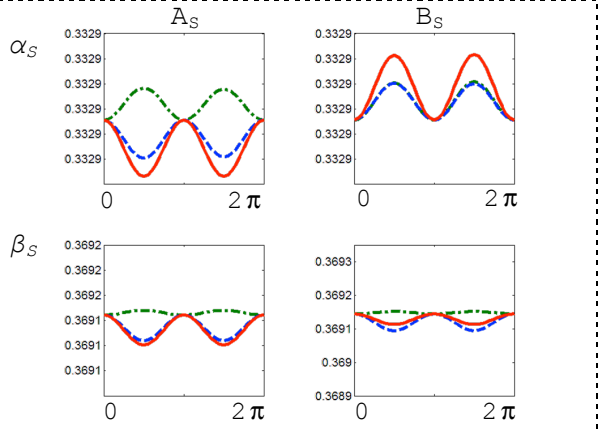

Figure 1.a Modulation of the symmetric optical modes, evolution of the reduced optical frequency (ωa/2πc) along one acoustic period (Ωt) from 0 to 2π of modes A_S and B_S respectively.

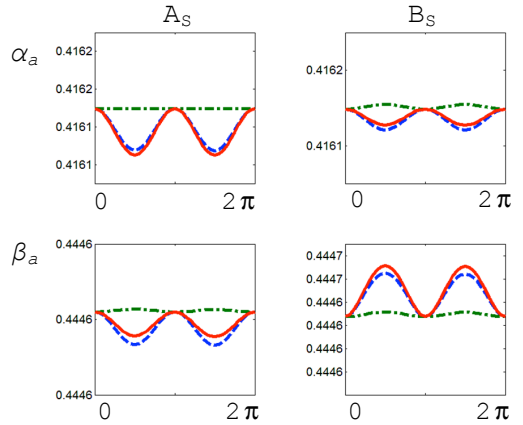

Figure 1.b Modulation of anti-symmetric optical modes, evolution of the reduced optical frequency (ωa/2πc) along one acoustic period (Ωt) from 0 to 2π of modes A_S and B_S respectively.

4. Concluding remarks

Acousto-optic coupling phenomena in dual photonic and phononic crystal slabs are studied. More specifically, the modulation of the optical eigenfrequences under the perturbation of the acoustic eigenmodes of a L_1 cavity is depicted. The global modulation of the frequency of the optical modes is strongly dependant on the choice of the modulating acoustic mode; upon this the photo-elastic and opto-mechanic effects can sustain each other or act with counteracted effects. The complexity of the acoustic modes of the slab does not evidence a fully symmetric mode; consequently the modulation of the optical eigenfrequencies is only possible at twice the acoustic frequency. This study can be useful to design phoxonic acousto-optic modulators.

[1] Yablonovitch E, 1987 *Phys. Rev. Lett.* **58** 2059
[2] Kushwaha MS et al., 1993 *Phys. Rev. Lett.* **71** 2022
[3] Lin TR et al., 2013 *Appl. Phys. Lett.* **113** 053508
[4] Papanikolaou N et al., 2012 *Microelec. Eng.* **90** 155
[5] Pennec Y et al., 2010 *Opt. Ex.*. **18** 14301
[6] Rolland Q et al., 2012 *Appl. Phys. Lett.* **101** 061109
[7] Rosencher E, Vinter B, Optoélectronique, *Masson* Paris Milan Barcelone
[8] Chan J et al., 2012 *Appl. Phys. Lett.* **101** 081115